

Goos–Hänchen effect in semiconductor metamaterial waveguide and its application as a biosensor

Tingting Tang¹ · Chaoyang Li² · Li Luo¹ · Yanfen Zhang¹ · Jie Li¹

Received: 17 March 2016 / Accepted: 14 May 2016 / Published online: 31 May 2016
© Springer-Verlag Berlin Heidelberg 2016

Abstract We investigate Goos–Hänchen (GH) effect in a prism waveguide coupling structure with semiconductor metamaterial (SMM) of ZnGaO/ZnO multilayer and explore the possibility as a biosensor. The GH effect in three different waveguides and their performances as a refractive index sensor to detect glycerol concentration in water are analyzed. The SMM brings a periodic property of GH shift peaks which is not found in other waveguides. It is also verified that setting coupling layer of the prism waveguide coupling structure as sensing area is an effective method to significantly increase the sensitivity to refractive index variation. A schematic diagram for the biosensor configuration is designed, and the sensitivity distribution for different glycerol water index is given. Calculation results show that in the proposed biosensor the maximum sensitivity reaches $3.2 \times 10^6 \mu\text{m}/\text{RIU}$ and resolution reaches 1.6×10^{-7} (around 1.33306) with high sensitive position sensitive detector.

1 Introduction

Goos–Hänchen (GH) shift is a lateral shift of the reflected light beam that occurs from the position predicted by geometrical optics when a light beam is totally reflected at a dielectric interface [1, 2]. In an ordinary case, the GH

shift is of the order of one wavelength, which impedes its direct observation in a single reflection. Recently, the enhancement of GH shift has attracted much attention of researchers and large lateral shift has been realized in different structures for its potential applications in integrated optics, optical storage and optical sensors. Many methods are utilized to realize an enhanced GH effect such as leaky guided mode generation in a thin dielectric layer [3], a Kretschmann configuration with long-range surface plasmon resonance (SPR) [4], magneto-optic enhancement in prism waveguide coupling structure [5] and multilayered waveguide with hyperbolic metamaterials (HMMs) [6].

HMM is a kind of metamaterial [7, 8] which have become a topic of significant research interest in recent years [9–11]. It is formed by stacks of alternating, sub-wavelength thin metallic and dielectric layers which can be regarded as an effective uniaxial crystal. HMMs based on semiconductors with InGaAs/AlInAs multilayers show negative refractive index in mid-infrared region [12]. In 2012, Naik et al. [13] proposed a HMM in the near-infrared spectral range at about $1.9 \mu\text{m}$ using ZnAlO/ZnO. HMMs operating at telecommunication wavelengths using heavily doped ZnGaO as plasmonic component are demonstrated by Kalusniak et al. [14] which have attractive applications in imaging below the diffraction limit with telecommunication light. For simplicity, we call this kind of HMM with ZnGaO/ZnO multilayer as semiconductor metamaterial (SMM).

In this paper, we first investigate the GH effect in a prism waveguide coupling structure with SMM and explore its application as a highly sensitive biosensor. Based on simulation results, GH effect in three different waveguides and their performances as a refractive index sensor to detect glycerol concentration in water are analyzed.

✉ Tingting Tang
skottt@163.com

¹ Information Materials and Device Applications Key Laboratory of Sichuan Provincial Universities, Chengdu University of Information Technology, Chengdu 610225, China

² Solorein Technology Inc, Chengdu 610209, China

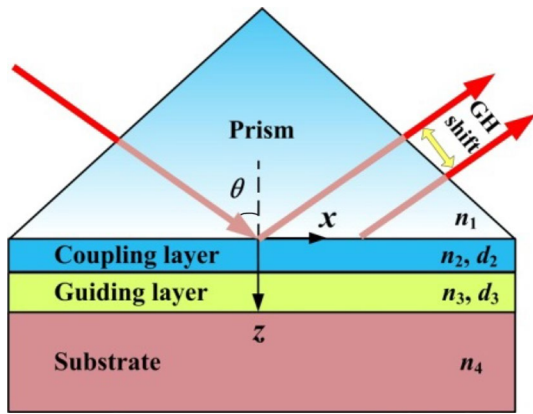


Fig. 1 Schematic of the prism waveguide coupling structure

2 Principle and theoretical analysis

The proposed prism waveguide coupling structure is shown in Fig. 1, which consists of prism, coupling layer, guiding layer and substrate. The refractive index of each layer is n_i ($i = 1, 2, 3, 4$), and the thicknesses of coupling layer and guiding layer are d_2 and d_3 , respectively.

Here we choose the SMM as the guiding layer which has an anisotropic permittivity of

$$\epsilon_2 = \begin{pmatrix} \epsilon_{\parallel} & & \\ & \epsilon_{\parallel} & \\ & & \epsilon_{\perp} \end{pmatrix} \quad (1)$$

According to the dispersion relation of SMM, we can get [14]

$$\epsilon_{\parallel} = \frac{\epsilon_{\text{ZnGaO}}\epsilon_{\text{ZnO}}}{\rho\epsilon_{\text{ZnO}} + (1 - \rho)\epsilon_{\text{ZnGaO}}} \quad (2)$$

$$\epsilon_{\perp} = \rho\epsilon_{\text{ZnGaO}} + (1 - \rho)\epsilon_{\text{ZnO}} \quad (3)$$

where $\epsilon_{\text{ZnO}} = 3.7$ and $\rho = d_{\text{ZnGaO}}(d_{\text{ZnGaO}} + d_{\text{ZnO}})^{-1}$. The permittivity of ZnGaO is described by Drude's dielectric function

$$\epsilon_{\text{ZnGaO}} = \epsilon_{\text{ZnO}} - \frac{\omega_p^2}{\omega(\omega + i\Gamma)} \quad (4)$$

in which ω_p is the plasma frequency and Γ is electronic damping rate. Here we choose $\hbar\omega_p = 1.88$ eV and $\Gamma = 112$ meV. The SMM consists of 20 pairs of ZnO/ZnGaO with an individual layer thickness of $d_{\text{ZnO}} = 45$ nm and $d_{\text{ZnGaO}} = 40$ nm. The total thickness of SMM is 1.7 μm .

According to the stationary-phase approach, the lateral beam shift is given by [15]

$$L = -\frac{1}{k} \cdot \frac{d\phi}{d\theta} \quad (5)$$

where $\phi = a \tan \left(\frac{\text{Im}(ND^*)}{\text{Re}(ND^*)} \right)$, N and D^* represent the numerator and the complex conjugate of denominator of r_{1234} . The reflection coefficient of the four-layer optical system can be written as [15]

$$r_{1234} = \frac{r_{12} + r_{12}r_{23}r_{34} \exp(2ik_{3z}d_3) + [r_{23} + r_{34} \exp(2ik_{3z}d_3)] \exp(2ik_{2z}d_2)}{1 + r_{23}r_{34} \exp(2ik_{3z}d_3) + r_{12}[r_{23} + r_{34} \exp(2ik_{3z}d_3)] \exp(2ik_{2z}d_2)} \quad (6)$$

with

$$r_{ij} = \begin{cases} \frac{k_{iz}/\epsilon_i - k_{jz}/\epsilon_j}{k_{iz}/\epsilon_i + k_{jz}/\epsilon_j} & \text{p-polarized wave} \\ \frac{k_{iz} - k_{jz}}{k_{iz} + k_{jz}} & \text{s-polarized wave} \end{cases} \quad (7)$$

where r_{ij} is the Fresnel reflection coefficient at the interface of layer i and layer j ; k_{iz} is the z component of the wave vectors in layer i , which can be expressed as $k_{iz} = k_0 \sqrt{\epsilon_i \mu_i - k_x^2}$, where k_x is the x component of the wave vector and k_0 is the vacuum wave vector of the incident light. As SMM is anisotropic, k_{2z} can be written as

$$k_{2z}^p = \sqrt{k_0^2 \epsilon_{\parallel} - \frac{\epsilon_{\parallel}}{\epsilon_{\perp}} k_x^2} \text{ and } k_{2z}^s = \sqrt{k_0^2 \epsilon_{\parallel} - k_x^2}. \text{ We can get}$$

$$r_{12}^p = \frac{k_{1z}/\epsilon_1 - k_{2z}/\epsilon_{\parallel}}{k_{1z}/\epsilon_1 + k_{2z}/\epsilon_{\parallel}} \quad (8)$$

$$r_{23}^p = \frac{k_{2z}/\epsilon_{\parallel} - k_{3z}/\epsilon_3}{k_{2z}/\epsilon_{\parallel} + k_{3z}/\epsilon_3} \quad (9)$$

3 Simulation results and discussion

In the following simulation, we assume a p-polarized wave is injected into the prism waveguide coupling structure. We choose BK7 glass as the prism with a dispersion relation of

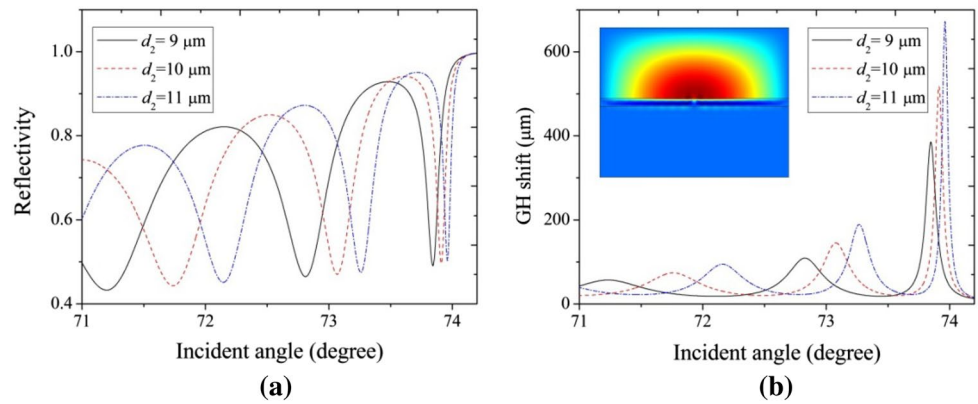
$$n_1 = \sqrt{1 + \frac{1.040\lambda^2}{\lambda^2 - 0.006} + \frac{0.232\lambda^2}{\lambda^2 - 0.020} + \frac{1.010\lambda^2}{\lambda^2 - 103.561}} \quad (10)$$

In this section, we study the GH effect in different waveguides to realize a biosensor with high sensitivity for glycerol concentration detection.

3.1 Prism/silica/SMM/water waveguide

We first choose a waveguide with prism/silica/SMM/water in which $\lambda = 1.55$ μm , $n_1 = 1.5007$, $n_2 = 1.444$, $\epsilon_{\parallel} = 1.154 + 0.3562i$, $\epsilon_{\perp} = -4.8497 + 5.6774i$ and $n_4 = 1.333$. The reflectivity and GH shift for different coupling layer thickness are shown in Fig. 2a, b, respectively. We can find in the proposed waveguide with SMM, the reflectivity shows periodic small-value peaks at different incident angle. It is not found in ordinary plasmonic waveguide in which only one reflectivity peak appears. When the

Fig. 2 The reflectivity and GH shift for different d_2 in prism/silica/SMM/water waveguide



reflectivity is minimum, the incident light is coupled into the waveguide and guiding mode in the three-layer waveguide is excited. The reflectivity peak is narrowed dramatically with the increase of incident angle. Meanwhile, the corresponding GH shift is dramatically increased at a narrowed reflectivity peak. This is because a sharp peak of reflectivity means a rapid and strong coupling of light into the waveguide. It can also be regarded as a deeper penetration depth of light along z -axis. As GH shift peak is proportional to the penetration depth of light, GH effect can be greatly enhanced when sharper reflectivity appears in angular spectrum.

In order to find the light energy distribution where light is coupled into the waveguide, the electrical field distribution of guiding mode in the z -axis of the silica/MM/water waveguide is given in the inset in Fig. 2b in which $d_2 = 10 \mu\text{m}$. It is easy to see that the incident light energy is mainly concentrated in the coupling layer. Thus, it may be insensitive to the refractive index change of water with different glycerol concentration. In addition, with the increase of d_2 the reflectivity peak has a shift to a larger incident angle and the GH shift is also enlarged.

In addition, we can find the reflectivity spectrum for mode at around 74° degree is much sharper than that for mode at around 73° . This means when incident angle is around 74° , the incident light is coupled into the guiding layer more rapidly and a guiding mode is generated. The field distributions for these two modes are certainly different. However, in our study, we mainly focus on the location of energy distribution which affects the sensitivity to refractive index variation. Therefore, in our paper we did not give the field distribution for different modes.

Then, we study the spectral characteristic of GH shift in the proposed waveguide as SMM is strongly dispersive. We assume the dispersion relation of silica is described by Hoffman et al. [12]

$$n_2 = \sqrt{1 + \frac{0.696\lambda^2}{\lambda^2 - 0.005} + \frac{0.408\lambda^2}{\lambda^2 - 0.014} + \frac{0.8974794\lambda^2}{\lambda^2 - 97.934}} \quad (11)$$

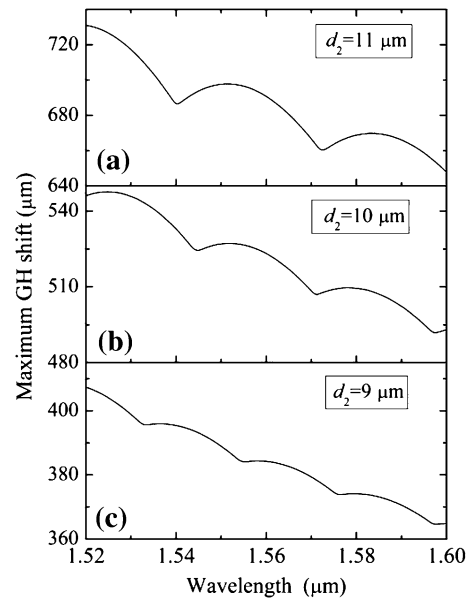


Fig. 3 The spectral characteristic of GH shift

In order to illustrate the GH shift peak variation, we give the maximum GH shift as shown in Fig. 3. In fact, the incident angles for maximum GH shifts in Fig. 3 are different for different wavelength and silica thickness. In our calculation, we choose the incident angle is in a range of 73.5° – 74.5° in which the maximum GH shift is given in Fig. 3. Thus, in our results we only need to record the maximum GH shift value rather than the incident angle. In the following simulation, we make use of the maximum GH shift variation to detect the refractive index variation as shown in Fig. 4. In this course, we also do not care the incident angle at which the maximum GH shift appears. We can find with the increase of incident wavelength, the GH shift peak is dramatically decreased. The spectral curves of GH shift show a periodic trend which is induced by the dispersion of SMM. This periodic property of GH shift has not been found in other waveguide to our knowledge. It can be

explained as the periodic resonance of SMM for different wavelength brings periodic coupling of light into the waveguide. Thus, periodic GH peaks appear in the spectrum. In addition, the increase of d_2 also brings an enhancement of GH effect. This means a larger coupling layer thickness confines the light energy better in the waveguide. When light is coupled into the waveguide, the guiding mode can propagate a relative longer distance. Thus, when the coupling layer thickness increases, the GH shift peak also increases at the same incident wavelength.

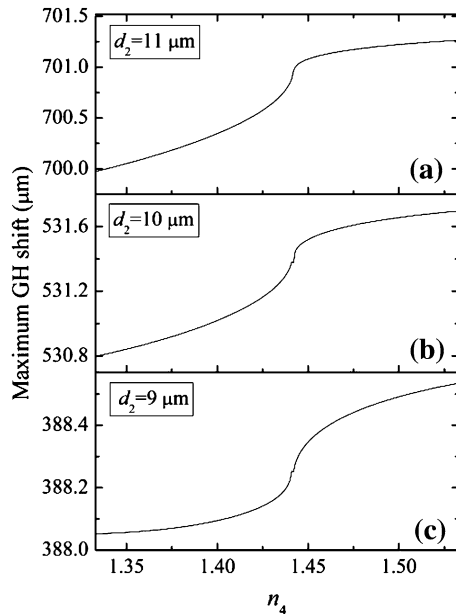


Fig. 4 The maximum GH shift distribution in for different d_2 in prism/silica/MM/water prism/silica/SMM/analyte for different waveguide refractive index of glycerol water when d_2 is different

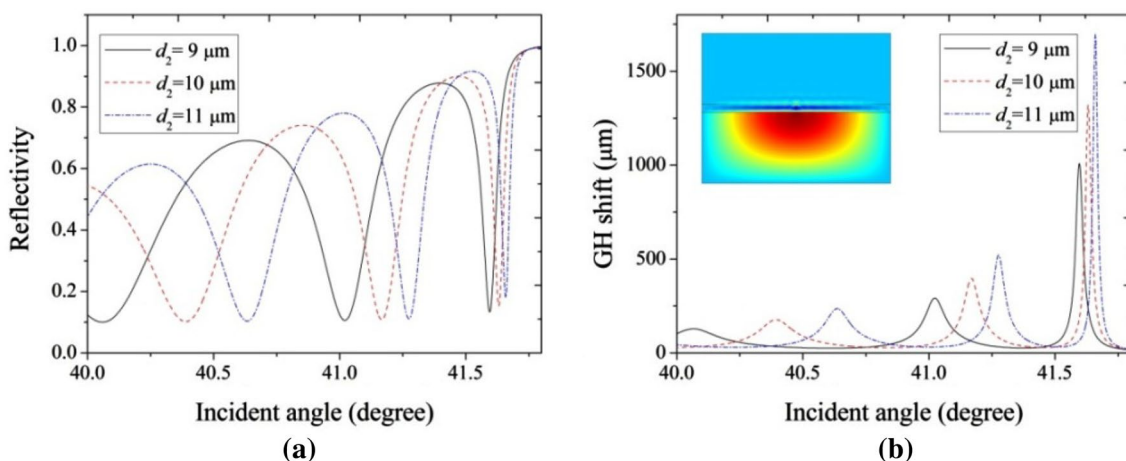


Fig. 5 The reflectivity and GH shift for different d_2 in prism/air/SMM/water waveguide

In the following, we make use of glycerol water to replace pure water in the prism waveguide coupling structure to realize a refractive index sensor. The maximum GH shift variation with the increase of glycerol water index is shown in Fig. 4. We can find a refractive index change of 0.2 only brings a GH shift peak variation range of $<1.5 \mu\text{m}$ when $d_2 = 11 \mu\text{m}$. This value still decreases with the decrease of coupling layer thickness. Such a small variation of GH shift peak in a relative large change of glycerol water concentration is obviously not suitable to be applied as a biosensor. Therefore, we should take measures to improve the sensitivity of the prism waveguide coupling structure as a refractive index sensor.

3.2 Prism/air/MM/water waveguide

In this section, we replace the silica layer with air to concentrate light energy in water. We also choose $\lambda = 1.55 \mu\text{m}$, $n_1 = 1.5007$, $n_2 = 1.0$, $\varepsilon_{\parallel} = 1.154 + 0.3562i$, $\varepsilon = -4.8497 + 5.6774i$ and $n_4 = 1.333$. The reflectivity and GH shift for different coupling layer thickness are shown in Fig. 5a, b, respectively. The inset in Fig. 5b shows most of the coupled incident light is distributed in the water layer when $d_2 = 10 \mu\text{m}$ which may bring an enhancement of sensitivity to the refractive index variation. Compared with Fig. 2, the incident angle corresponding to GH shift peak is dramatically reduced. This phenomenon can be explained as the effective refractive index of guiding mode is affected by the waveguide parameters. It is known that when the incident light is coupled into the waveguide, the guiding mode is excited. When the coupling layer is replaced by air, the guiding mode index and effective propagation constant are also reduced. According to the phase-matching condition, the propagation constant is

always equal to $k_0 n_1 \sin \theta$. Thus, the reduction of propagation constant brings a decrease of critical incident angle. Therefore, the GH shift peak appears at a smaller incident angle. In addition, we can find with the same SMM thickness the maximum GH shift is increased by over twice than that in Fig. 2.

The spectral characteristic of GH shift for different d_2 in prism/air/MM/water waveguide is almost the same as in Fig. 3; thus, we do not mention it anymore. Then, we replace the pure water by glycerol water in the above waveguide to explore the sensitivity of the proposed structure as a biosensor. The maximum GH shift distribution for

different refractive index of glycerol water when d_2 is different is shown in Fig. 6. We can find although the maximum GH shift is greatly enlarged in this case, the sensitivity of the structure as a refractive index sensor is even weakened than in Fig. 4. With an increase of glycerol water index, the GH shift peak variation range is about $0.4 \mu\text{m}$ for $d_2 = 9 \mu\text{m}$. Even for $d_2 = 11 \mu\text{m}$, a refractive index change of 0.2 only brings a GH shift variation of $<1.0 \mu\text{m}$. Therefore, the proposed structure is also not suitable for a highly sensitive biosensor.

3.3 Prism/water/MM/air waveguide

At last we exchange the locations of water and air in the above waveguide to realize a sensitive biosensor. Here we also choose the same parameters as in Fig. 5. The reflectivity and GH shift for different d_2 in prism/water/SMM/air waveguide are shown in Fig. 7a, b, respectively. In this case, the maximum GH shift is smaller than that in Fig. 5 with the same d_2 . Compared with Fig. 5, the incident angle corresponding to GH shift peak becomes from about 42° to 62.5° . As is known to us, the effective refractive index of guiding mode in Figs. 5 and 6 should be identical. But we also find the critical angle of GH shift peak still has an obvious shift to larger value. This phenomenon is induced by different coupling layer in the two waveguides. A coupling layer with small refractive index contributes more to the enhancement of GH shift. In addition, the light energy distribution in the waveguide when $d_2 = 10 \mu\text{m}$ is shown in the inset of Fig. 7b. We can find most of the coupled light is concentrated in the water layer which is help to improve the sensitivity to refractive index.

Then, we replace the pure water by glycerol water in the above waveguide to detect the concentration of glycerol in water. The maximum GH shift variation with the increase of

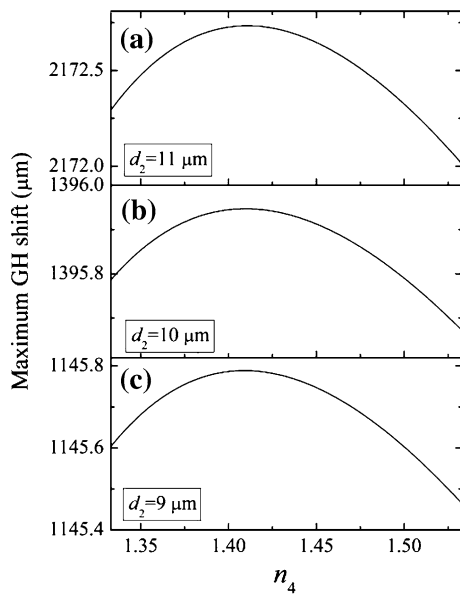


Fig. 6 The maximum GH shift distribution in prism/air/SMM/analyte for different refractive index of glycerol water when d_2 is different

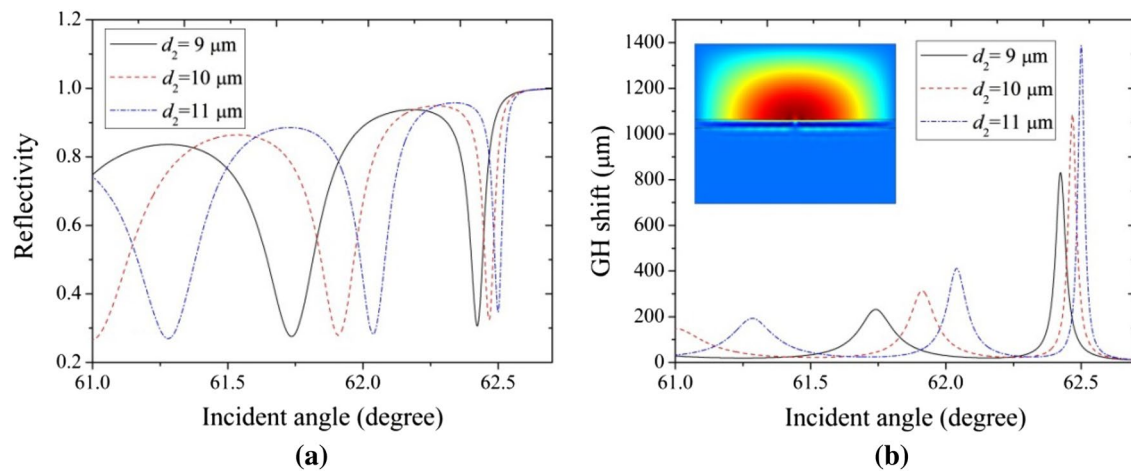


Fig. 7 The reflectivity and GH shift for different d_2 in prism/water/SMM/air waveguide

glycerol water index for different d_2 is shown in Fig. 8. When the thickness of glycerol water is increased, the GH shift also increases which is similar to the situation in the above two waveguides. In this configuration, the most important difference is that the GH shift peaks show a periodic property. Meanwhile, the amplitude of the GH shift peak variation is almost unchanged for different refractive index of glycerol water. We can find a small refractive index change of 0.0001 in the coupling layer may bring a GH shift peaks variation of more than 250 μm for $d_2 = 11 \mu\text{m}$ which can be further enlarged by the increase of sensing area thickness. In this

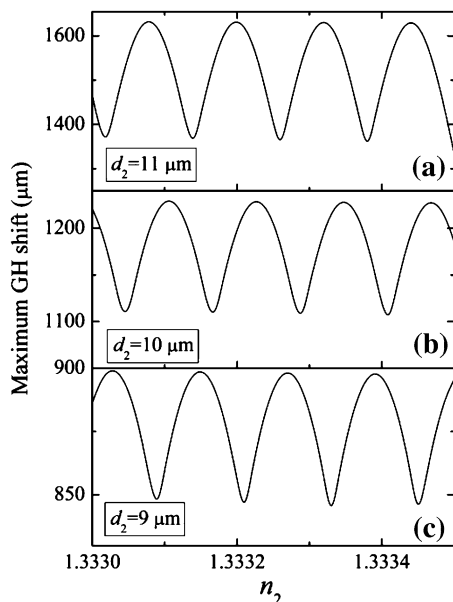
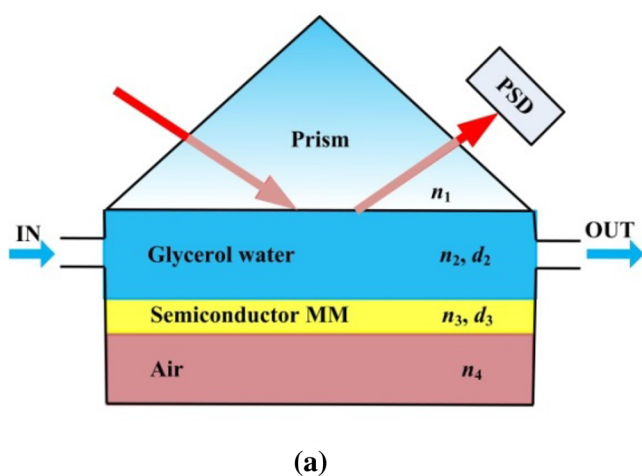


Fig. 8 The maximum GH shift distribution in prism/analyte/SMM/air for different refractive index of glycerol water when d_2 is different



configuration, the sensitivity as a refractive index sensor can be significantly increased compared with the above two waveguides. In the following, we design a possible biosensor diagram and estimate the sensitivity and resolution based on the proposed prism/water/SMM/glycerol water waveguide.

Here we set the coupling layer as the sensing area and design a microfluidic channel to input the glycerol water to be detected as shown in Fig. 9a. The glycerol water is injected into the measurement cavity from the “IN” port and then exported from the “OUT” port. When a light beam is incident into the prism, the reflected light is detected by position sensitive detector (PSD). Then, the GH shift peak variation induced by glycerol water with different concentrations can be obtained. The GH shift can be detected by PSD. Here we define the sensitivity as

$$S = \frac{dL_{\text{max}}}{dn_2} \tag{12}$$

The sensitivity of the configuration for $d_2 = 10 \mu\text{m}$ as a refractive index sensor is shown in Fig. 9b. We can find the maximum sensitivity of the biosensor reaches $3.2 \times 10^6 \mu\text{m}/\text{RIU}$. Further calculation shows if the resolution of PSD is 0.5 μm , the proposed biosensor can detect even a refractive index variation (around 1.33306) as small as 1.6×10^{-7} . This means glycerol concentration changes as small as 0.1 mg/dL. Compared with ordinary biosensor based on short-range surface plasmon excitation, the sensitivity is improved by one order of magnitude [16].

4 Conclusion

In this paper, we investigate GH effect in a prism waveguide coupling structure with SMM and explore the

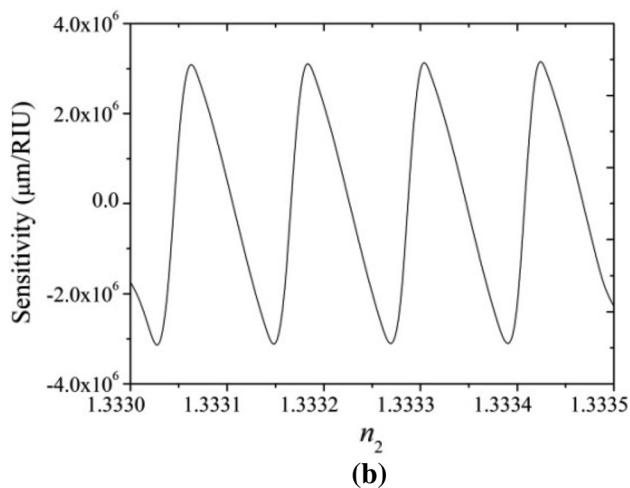


Fig. 9 **a** Schematic diagram of the biosensor configuration and **b** sensitivity as a refractive index sensor

possibility as a biosensor. As SMM is anisotropic whose permittivity components are partially negative, it brings a high flexibility for the modulation of GH shift as well as the design as a biosensor. The GH effect in three different waveguides and their performances as a refractive index sensor to detect glycerol concentration in water are analyzed based on simulation results. The SMM brings a periodic property of GH shift peaks which is not found in other waveguides. We find that setting coupling layer as the sensing area can significantly improve the sensitivity to refractive index variation. We also design a schematic diagram for the biosensor configuration and derive the sensitivity distribution for different glycerol water index. Calculation results show that in the proposed biosensor maximum sensitivity reaches $3.2 \times 10^6 \mu\text{m}/\text{RIU}$ and resolution reaches 1.6×10^{-7} (around 1.33306) with highly sensitive PSD.

Acknowledgments This work is supported by the National Natural Science Foundation of China under Grant No. 61505016, the project of Sichuan Provincial Department of Education (15ZA0183) and the scientific research fund of Chengdu University of Information Technology (No. J201417).

References

1. F. Goos, H. Hänchen, Ein neuer und fundamentaler Versuch zur Totalreflexion. *Ann. Phys.* **1**, 333–346 (1947)
2. F. Bretenaker, A. Le Floch, L. Dutriaux, Direct measurement of the optical Goos–Hänchen effect in lasers. *Phys. Rev. Lett.* **68**, 931–933 (1992)
3. F. Pillon, H. Gilles, S. Girard, M. Laroche, Goos–Hänchen and Imbert–Fedorov shifts for leaky guided modes. *J. Opt. Soc. Am. B* **6**, 1290–1299 (2005)
4. H.F. Wang, Z.X. Zhou, H. Tian, D.J. Liu, Y.Q. Shen, Electric control of enhanced lateral shift owing to surface Plasmon resonance in Kretschmann configuration with an electro-optic crystal. *J. Opt.* **12**, 045708 (2010)
5. T. Tang, J. Qin, J. Xie, L. Deng, L. Bi, Magneto-optical Goos–Hänchen effect in a prism-waveguide coupling structure. *Opt. Express* **22**, 27042–27055 (2014)
6. C.-W. Chen, T. Bian, H.-P. Chiang, P.T. Leung, Nonlocal optical effects on the Goos–Hänchen shifts at multilayered hyperbolic metamaterials. *J. Opt.* **18**, 025104 (2016)
7. V.G. Veselago, The electro-dynamics of substances with simultaneously negative values of ϵ and μ . *Sov. Phys. Usp.* **10**, 509–513 (1968)
8. J.B. Pendry, Negative refraction makes a perfect lens. *Phys. Rev. Lett.* **85**(18), 3966–3969 (2000)
9. A. Poddubny, I. Iorsh, P. Belov, Y. Kivshar, Hyperbolic metamaterials. *Nat. Photonics* **7**(12), 948–957 (2013)
10. P. Shekhar, J. Atkinson, Z. Jacob, Hyperbolic metamaterials: fundamentals and applications. *Nano Converg.* **1**(1), 14 (2014)
11. L. Ferrari, C. Wu, D. Lepage, X. Zhang, Z. Liu, Hyperbolic metamaterials and their applications. *Prog. Quantum Electron.* **40**, 1–40 (2015)
12. A.J. Hoffman, L. Alekseyev, S.S. Howard, K.J. Franz, D. Wasserman, V.A. Podolskiy, E.E. Narimanov, D.L. Sivco, C. Gmachl, Negative refraction in semiconductor metamaterials. *Nat. Mater.* **6**(12), 946–950 (2007)
13. G.V. Naik, J. Liu, A.V. Kildishev, V.M. Shalaev, A. Boltasseva, Demonstration of Al:ZnO as a plasmonic component for near-infrared metamaterials. *Proc. Natl. Acad. Sci. USA* **109**(23), 8834–8838 (2012)
14. S. Kalusniak, L. Orphal, S. Sadofev, Demonstration of hyperbolic metamaterials at telecommunication wavelength using Gadoped ZnO. *Opt. Express* **23**(25), 32555–32560 (2015)
15. L. Chen, X. Liu, Z. Cao, S. Zhuang, Mechanism of giant Goos–Hänchen effect enhance by long-range surface Plasmon excitation. *J. Opt.* **13**, 0350022011 (2011)
16. B. Fan, F. Liu, Y. Li, X. Wang, K. Cui, X. Feng, W. Zhang, Y. Huang, Integrated refractive index sensor based on hybrid coupler with short range surface plasmon polariton and dielectric waveguide. *Sens. Actuator B Chem.* **186**, 495–505 (2013)